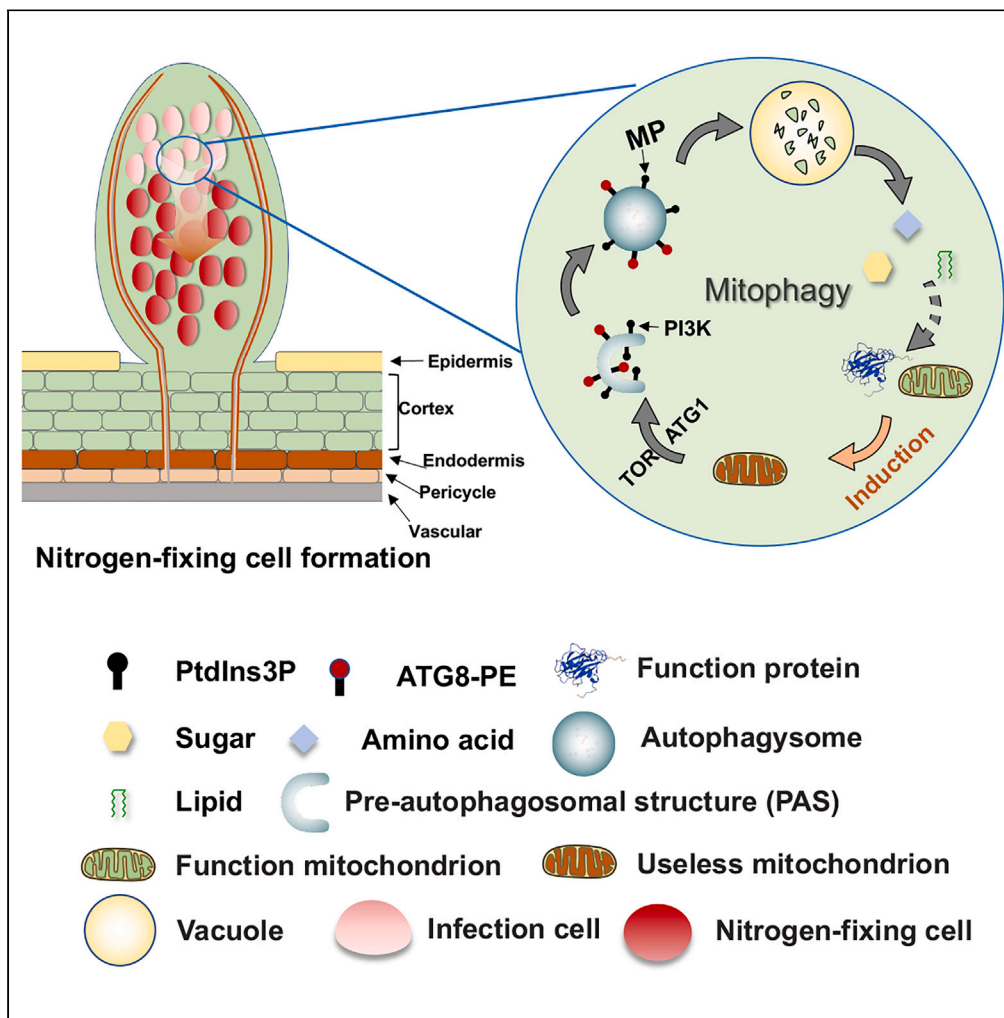


Article

The PtdIns3P phosphatase MtMP promotes symbiotic nitrogen fixation via mitophagy in *Medicago truncatula*



Qixia Xue, Chen Shen, Qianwen Liu, ..., Qinyi Ye, Tao Wang, Jiangli Dong

dongjl@cau.edu.cn

Highlights
MtMP dephosphorylates PtdIns3P on autophagosomes

MtMP promotes autophagosomes fusion with vacuoles

MtMP promotes symbiotic nitrogen fixation via mitophagy in legumes

Xue et al., iScience 26, 107752
October 20, 2023 © 2023 The Authors.
<https://doi.org/10.1016/j.isci.2023.107752>



Article

The PtdIns3P phosphatase MtMP promotes symbiotic nitrogen fixation via mitophagy in *Medicago truncatula*Qixia Xue,^{1,2} Chen Shen,^{1,2} Qianwen Liu,¹ Peng Liu,¹ Da Guo,¹ Lihua Zheng,¹ Jinling Liu,¹ Chang Liu,¹ Qinyi Ye,¹ Tao Wang,¹ and Jiangli Dong^{1,3,*}

SUMMARY

Symbiotic nitrogen fixation is a complex process in which legumes interact with rhizobia under nitrogen starvation. In this study, we found that myotubularin phosphatase (MtMP) is mainly expressed in roots and nodules in *Medicago truncatula*. MtMP promotes autophagy by dephosphorylating PtdIns3P on autophagosomes. The *mp* mutants inoculated with rhizobia showed a significant reduction in nitrogenase activity and significantly higher number of mitochondria than those of wild-type plants under nitrogen starvation, indicating that MtMP is involved in mitophagy of the infection zone. Mitophagy may provide carbon skeletons and nitrogen for the development of bacteroids and the reprogramming of infected cells. In conclusion, we found, for the first time, that myotubularin phosphatase is involved in autophagy in plants. MtMP-involved autophagy plays an active role in symbiotic nitrogen fixation. These results deepen our understanding of symbiotic nitrogen fixation.

INTRODUCTION

Autophagy is an important “self-eating” process that recycles waste proteins as well as organelles such as mitochondria, chloroplasts, and proteasomes during normal life processes and stress responses.^{1–3} When cells require autophagy, TOR, an important kinase involved in the upstream negative regulation of autophagy, is inactivated, and the assembly of the ATG1 kinase complex induces autophagy initiation.⁴ Next, lipid delivery to expanding autophagic vesicles is driven by the transmembrane protein ATG9 and its recycling factors ATG2 and ATG18.⁵ The PI3K kinase complex modifies autophagic vesicles by phosphorylating PtdIns to PtdIns3P in the midstream regulation of autophagy.⁶ The next step is that the ATG8-PE complex covers expanding autophagic vesicles, and ATG8- and PtdIns3P-coated autophagosomes are transported to vacuoles.⁷ Then, proteins downstream of autophagy, such as FREE1, are involved in the fusion between the outer membrane of autophagosomes and the vacuole membrane, thereby releasing the autophagosome.⁸ Once the autophagosome enters the vacuole, the inner membrane of the autophagosome and its cargos are degraded by vacuole hydrolases.¹

Myotubularin phosphatase dephosphorylates PtdIns3P.⁹ Myotubularin phosphatase are known to play a fundamental role in human physiology, and deletion of these genes can lead to a variety of diseases.¹⁰ Myotubularin phosphatase is involved in the downstream process of autophagy by dephosphorylating PtdIns3P generated by PI3K in yeast, which in turn helps autophagosomes fuse with vacuoles.^{11–13} However, the involvement of the myotubularin phosphatase AtMTM1 and AtMTM2 in the regulation of reactive oxygen species (ROS) accumulation under drought stress has been reported in *Arabidopsis*.^{14,15} It is unknown whether myotubularin phosphatase is involved in autophagy in plants.

Symbiotic nitrogen fixation is a symbiotic and mutually beneficial relationship between rhizobia and legumes under nitrogen starvation, and the system involves several processes, such as infection thread formation, nodule primordia formation, and mature nitrogen fixation nodule formation.¹⁶ In legumes, PI3K and TOR, important regulatory genes in autophagy, regulate the process of rhizobial infection and the formation of nodule primordia. RNA interference (RNAi) of PI3K and TOR was shown to disrupt the formation of normal infection threads and functional nodules in plants.^{17,18} The infection threads of these RNAi-transformed plants were unable to penetrate the root cortex cells, and it was difficult to form normal nodules. However, whether autophagy is involved in the formation of mature root nodules, has not been reported.

In this study, we identified a myotubularin phosphatase, MtMP, in *Medicago truncatula*. MtMP is involved in autophagy by dephosphorylating PtdIns3P on autophagosomes. The MtMP expressed in the infection zone of nodules promotes nitrogen fixation through mitophagy.

¹College of Biological Sciences, China Agricultural University, Beijing, China

²These authors contributed equally

³Lead contact

*Correspondence: dongjl@cau.edu.cn

<https://doi.org/10.1016/j.isci.2023.107752>



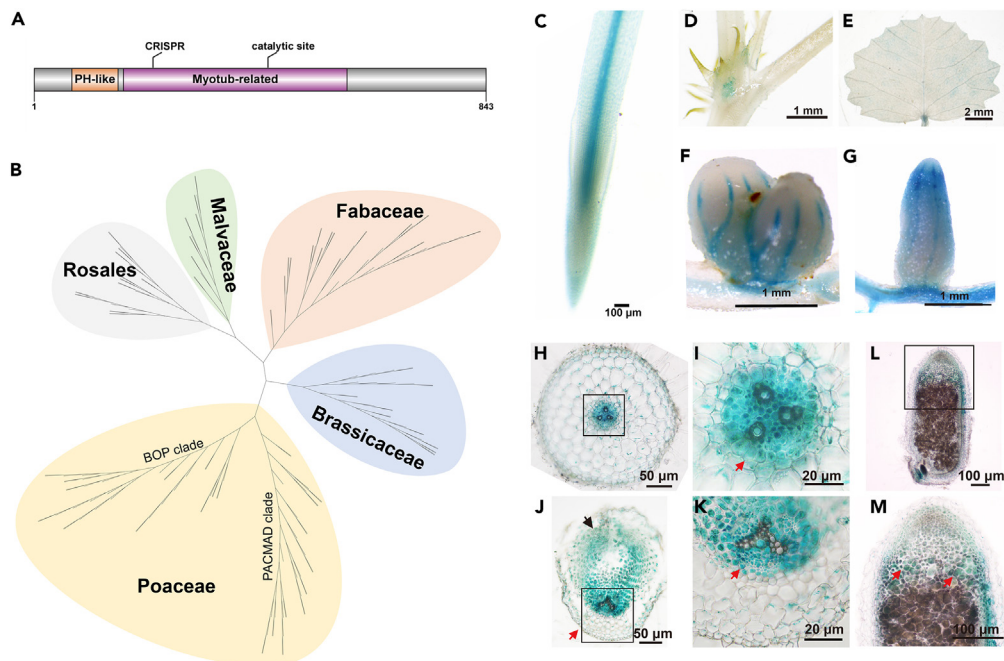


Figure 1. Phylogenetic analysis of myotubularin phosphatase and expression pattern of *MtMP*

(A) *MtMP* protein domains prediction plot. The CRISPR target is on the Myotub-related domain and before the catalytic site. Gray bar means protein skeleton. Orange bar means PH-like domain. Purple bar means myotub-related domain.

(B) The protein sequences of multi-species were used for phylogenetic analysis. Poaceae is the representative of monocotyledons, Rosales, malvaceae, fabaceae, and brassicaceae are the representative of dicotyledons. The original image with the protein ID is in the [Figure S1B](#).

(C–G) Gus staining of root (C), stem (D), leaf (E), 5 dpi nodule (F) and 21 dpi nodule (G) with *ProMP::GUS* plants (Bar = 100 μ m (C), 1 mm (D, F, G) and 2 mm (E)).

(H) Root cross section of *ProMP::GUS* plants (Bar = 50 μ m).

(I) Enlarged view of root cross section. Red arrows mean pericycle cells (Bar = 20 μ m).

(J) Early stage nodule (5dpi) cross section of *ProMP::GUS* plants. Black arrow means nodule-forming side of root. Red arrow means non-nodule-forming side of root (Bar = 50 μ m).

(K) Enlarged view of early stage nodule cross section. Red arrows mean pericycle cells (Bar = 20 μ m).

(L) Mature nodule (28dpi) cross section of *ProMP::GUS* plants (Bar = 100 μ m).

(M) Enlarged view of mature nodule cross section. Red arrows mean infection cells (Bar = 100 μ m)..

We speculate that mitophagy plays a crucial role in symbiotic nitrogen fixation. This study provides new ideas for understanding the regulatory mechanism underlying symbiosis between rhizobia and legumes.

RESULTS

Identification of *MtMP*

Myotubularin phosphatase gene *Ymr1* in yeast is able to participate in autophagy, and its mutants present partial inhibition of autophagy. We hope to find genes of the same family that perform similar functions in plants as well. Myotubularin phosphatase is commonly found in monocotyledons and dicotyledons by blast ([Figures 1B](#) and [S1B](#)). In dicotyledons, each family is a single branch, which is relatively conservative. While in Poaceae, the myotubularin family genes are divided into two distinct branches, and there may be functional divergence in different branches. In *Medicago truncatula* genome, there is only one myotubularin phosphatase, which we have named *MtMP*. And then we cloned *MtMP* from cDNA of *M. truncatula*. The coding sequence of *MtMP* is 2532 bp in length, and the *MtMP* protein consists of 843 amino acid residues, predicting to encode a 93 kDa protein. *MtMP* has two superfamily structural domains, the PH (pleckstrin homology)-like domain and the Myotube-related (myotubularin-like phosphatase) domain ([Figure 1A](#)). PH-like domains can bind to inositol phosphates and are often involved in directing proteins to appropriate cellular sites or interacting with binding proteins.¹⁹

Tissue expression pattern of *MtMP*

To determine the tissue expression localization of *MtMP*, we cloned the 2.5-kb promoter region sequence upstream of the ATG codon of the *MtMP* gene. *ProMP::GUS* transgenic plant material was constructed for GUS staining to detect *MtMP* tissue expression patterns, and the results showed deeper staining in roots and young nodules as well as mature nodules and lighter staining in leaves and stems ([Figures 1C–1G](#)).

To further clarify the expression of *MtMP* within the nodules, we performed agarose-embedded sections of GUS-stained roots, young nodules, and mature nodules. The results of root cross-sections showed that *MtMP* was localized in vascular bundle cells and pericycle cells, with no obvious staining in cortex cells (Figures 1H and 1I). At the early stage of nodule formation (5 days post inoculation (dpi)), *MtMP* was expressed in the infected cells of the nodule primordia and localized in vascular bundle cells and pericycle cells (Figure 1J). In the early stages of nodule development, pericycle cells are the first to differentiate, and then cortex cells differentiate and form nodules in symbiosis with rhizobia. Interestingly, we found that *MtMP* was expressed on the nodule-forming side of the root and not on the nonnodule side (Figures 1J and 1K), implying that *MtMP* plays a role in the process of nodule primordia division. At the nodule maturation stage (21 dpi), *MtMP* was expressed mainly in the infection zone of the nodules (Figures 1L and 1M). In summary, *MtMP* was mainly localized in the vascular tissue of the roots, the nodule primordia, and the infection zone of mature nodules.

To investigate the function of *MtMP* in depth, we constructed *MtMP* loss-of-function mutants. The myotube-related domain, the catalytic domain of the *MtMP* protein, was used as a clustered, regularly interspaced, short palindromic repeat (CRISPR)/CRISPR-associated 9 (Cas9) gene knockout target (Figure 1A). We used a modified CRISPR/Cas9 toolkit.²⁰ The T1 generation was obtained by self-crossing. Three *mp* mutant lines without the complete phosphatase active domain were finally screened (Figure S1A). We used *mp22* for all assays as its 41bp deletion can be checked easily, and three mutant lines for phenotype assays. All *mp* mentioned below are *mp22* except phenotype results.

MtMP can bind to and dephosphorylate PtdIns3P

Myotubularin is a bispecific lipid phosphatase that dephosphorylates PtdIns3P.²¹ Based on the function of the domain, we hypothesized that *MtMP* may bind to PtdIns3P and dephosphorylate PtdIns3P. To determine the lipid-binding capabilities of the *MtMP*, we purified the protein of *MtMP* PH-like domain fused with the His-MBP tag (His-MBP-MPN). And confirmed *MtMP* interact with PtdIns3P by protein lipid overlay assay (Figure 2A).

We use 2xFYVE to indicate PtdIns3P *in vivo*. 2xFYVE consists of two tandem FYVE domains that bind to PtdIns3P and can indicate the location of PtdIns3P *in vivo*.²² We used *Agrobacterium rhizogenes* ARqua1 to transform *Medicago truncatula*, and the mCherry-2xFYVE vector was expressed in WT and *mp* mutants to detect intracellular PtdIns3P. The GFP expression cassette in the expression vector was used as an internal reference to ensure consistent transgene efficiency. The results showed significant accumulation of 2xFYVE punctate fluorescence in the *mp* mutant (Figure 2B). The number of FYVE puncta in *mp* mutants was significantly greater than that in WT (Figure 2C), indicating that *MtMP* is able to dephosphorylate PtdIns3P *in vivo*.

Next, we assayed *MtMP* dephosphorylation activity *in vitro*. The myotubularin phosphatase AtMTM1 in *Arabidopsis* was used as a positive control for *in vitro* enzyme activity assays, as it has enzymatic activity and can dephosphorylate PtdIns3P. By referring to other myotubularin phosphatase activity confirmation methods,^{14,23} we purified the myotubule-related enzymatic activity domain for the enzyme activity assay. The results of the PtdIns3P phosphatase activity assay showed that *MtMP* has a distinct phosphate absorption peak compared to MBP blank control, similar to AtMTM1, indicating that *MtMP* has phosphatase activity *in vitro* (Figures 2D and S2). In summary, *MtMP* is a myotubularin phosphatase with enzymatic activity that can dephosphorylate PtdIns3P both *in vivo* and *in vitro*.

MtMP localizes to autophagosomes and participates in autophagy

Based on the fact that PtdIns3P binds to the autophagosome membrane¹ and our results that *MtMP* is able to dephosphorylate PtdIns3P, further research was conducted to investigate whether *MtMP* can participate in autophagy. ATG8 is a commonly used autophagy marker, and its punctate fluorescence in protoplasts can indicate the presence of autophagosomes. Coexpression of *MtMP*-GFP and mCherry-MtATG8 in *Arabidopsis* protoplasts shows that the fluorescence signal of *MtMP* could colocalize with the punctate fluorescence of ATG8 (Figure 3A). Similarly, *MtMP* was able to colocalize with the punctate fluorescence of 2xFYVE (Figure 3B). The above results indicated that *MtMP* localizes to autophagosomes.

Myotubularin phosphatase Ymr1 in yeast has been reported to participate in autophagy. We further investigated whether *MtMP* could play a role in the yeast *ymr1Δ* mutant. Autophagy complementation experiments were performed in *ymr1Δ* mutants using the transfer of *ProYmr1::MtMP* in yeast. The results of green fluorescent protein (GFP) cleavage experiments showed that the proportion of GFP remained unchanged in yeast *ymr1Δ* mutants due to the suppression of autophagy in *ymr1Δ* strains.¹² The proportion of GFP increased after *MtMP* transfer into the *ymr1Δ* mutant, and *MtMP* was able to complement the autophagy phenotype of the yeast *ymr1Δ* mutant (Figure S3). This result indicates that *MtMP* is functionally similar to Ymr1 in yeast and can play a role in promoting autophagy.

Whether *MtMP* is involved in nitrogen starvation-induced autophagy in *Medicago truncatula* was further investigated. We examined intracellular autophagy by transforming GFP-ATG8 into *Medicago truncatula* using ARqua1. After nitrogen starvation-induced autophagy, punctate fluorescence of ATG8 was significantly increased in *mp* mutants compared with WT, indicating an increase in autophagosomes (Figures 3C and 3D). As expected, a higher proportion of GFP-ATG8 and a lower proportion of cleaved GFP were found in the *mp* mutant than in the WT in the GFP cleavage assay (Figure 3E). This result indicates that autophagy is inhibited in *mp* mutants. Overall, the above results suggest that *MtMP* promotes autophagy in plants.

Autophagy is induced by nitrogen starvation and rhizobia

Legumes have a unique ability to nodulate and fix nitrogen. To further investigate the relationship between autophagy and symbiotic nodulation at the transcriptional level, we explored whether autophagy-related genes are involved in the early process of nitrogen starvation and nodulation symbiosis. We used RT-qPCR to examine the effects of nitrogen starvation and the inoculation of rhizobia on the expression of

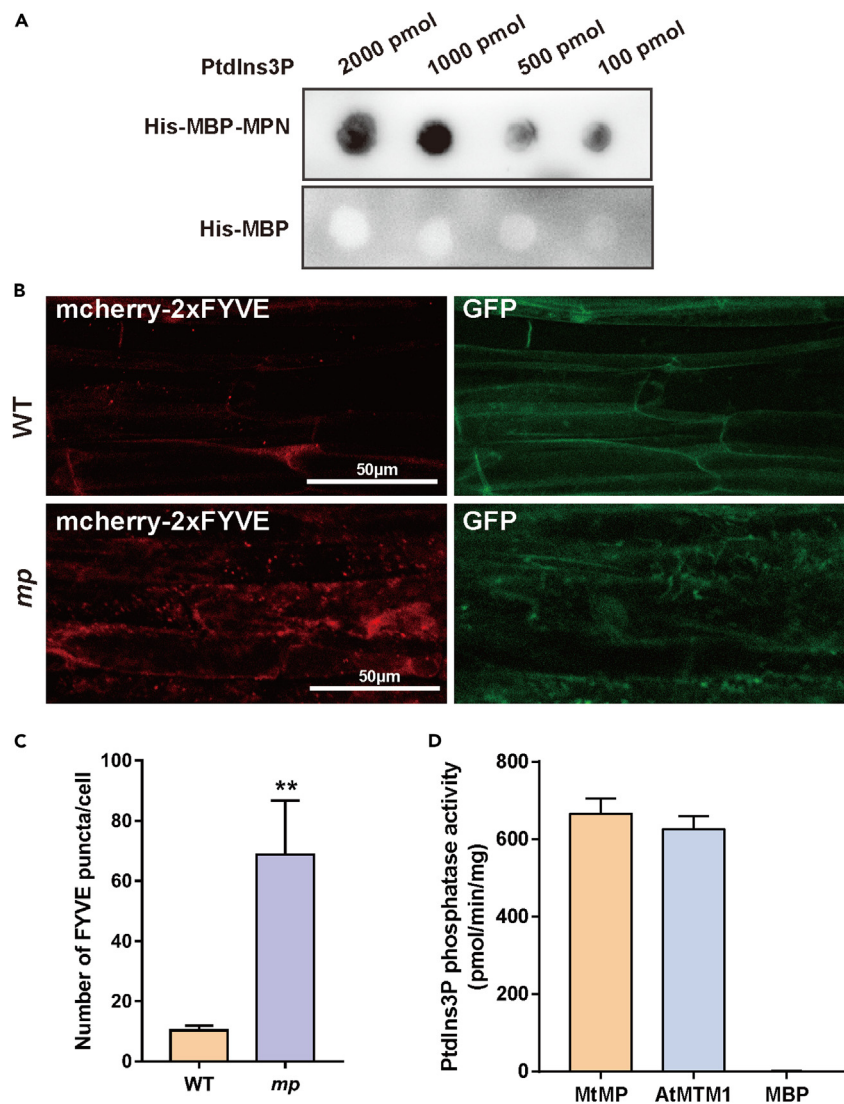


Figure 2. PtdIns3P phosphatase activity of MtMP

(A) Lipid protein overlay assay of recombinant MPN fused to His-MBP (His-MBP-MPN) with PtdIns3P.

(B) *Agrobacterium rhizogenes* *Aqua1* transforms mcherry-2xFYVE and GFP double expression vector into *Medicago* WT and *mp* mutant plants (Bar = 50 μ m). Left is mcherry-2xFYVE channel. Right is GFP channel.

(C) The number of FYVE puncta per cell in WT and *mp* mutant plants. Data are presented as mean \pm SD for 15 individual cells. ** $p < 0.01$ (Student's *t* test).

(D) PtdIns3P phosphatase activity of protein MtMP. AtMTM1 is regarded as positive control, and MBP empty vector as negative control.

autophagy-related genes. The results show that the expression of *TOR*, an important negative regulator upstream of autophagy, is significantly downregulated by nitrogen starvation and *Sm1021*. The expression of *ATG8*, *MtMP*, and *FREE1* downstream of autophagy was significantly upregulated (Figure 4). We also examined the GFP cleavage in GFP-*ATG8* transgenic *M. truncatula* nodulated roots after inoculation with *Sm1021* from 0 to 7 days. Immunoblot showed increased GFP cleavage after inoculation with *Sm1021* (Figure S4). The results indicated that autophagy is induced and activated in roots during nitrogen starvation and rhizobial infection.

MtMP promotes nitrogen fixation capacity

To explore the impact of MP deficiency on plant growth and development, we analyzed the phenotypes of WT and *mp* mutants under full nutrient conditions. There were no significant differences in *mp* mutants compared to WT in aboveground and underground parts under full nutrient conditions (Figure S5).

As found, both nitrogen starvation and *Sm1021* induction led to autophagy. *MtMP* high expressing in the underground parts is positively involved in autophagy. Therefore, we explored whether *MtMP* is involved in autophagy during nodulation. We found that *MtMP* affects the

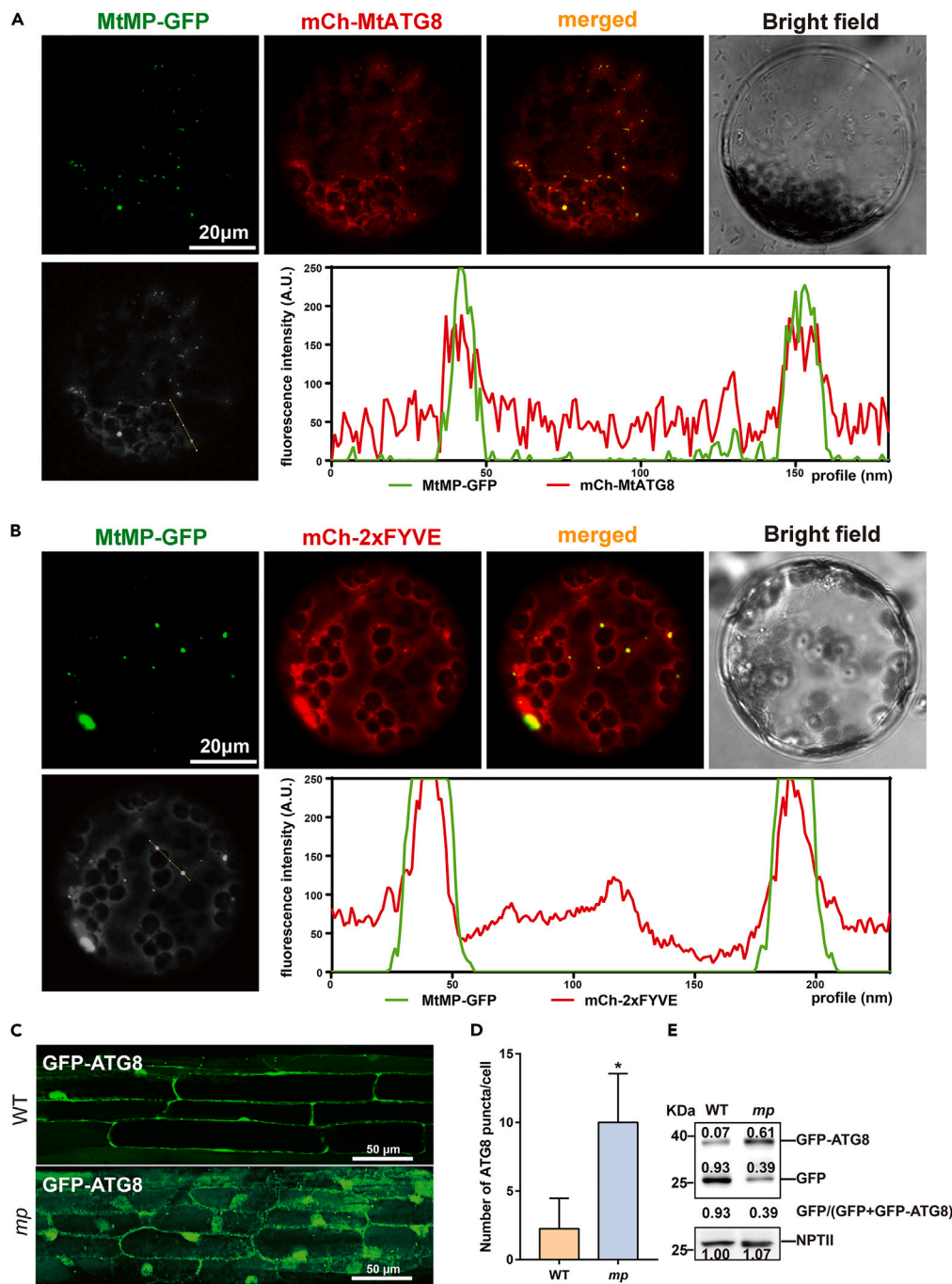


Figure 3. MP locate on autophagosomes and participates in autophagy

(A) Coexpression MtMP-GFP and mCherry-MtATG8 in *Arabidopsis* protoplast. The following figure is marked regions to calculate fluorescence intensity (Bar = 20 μ m).

(B) Coexpression MtMP-GFP and mCherry-2xFYVE in *Arabidopsis* protoplast. The following figure is marked regions to calculate fluorescence intensity (Bar = 20 μ m).

(C) *Agrobacterium rhizogenes* Aqua1 transforms GFP-ATG8 into *Medicago* WT and *mp* mutant plants (Bar = 50 μ m).

(D) Statistical analysis of the number of ATG8 puncta per cell in WT and *mp* mutant plants. * $p < 0.05$ (Student's *t* test).

(E) Immunoblotting quantitative analysis of GFP and GFP-ATG8 in WT and *mp* mutant plants transformed with GFP-ATG8. Numbers mean gray values of each lane and ratio of GFP and (GFP + GFP-ATG8). NPTII was used as internal reference gene.

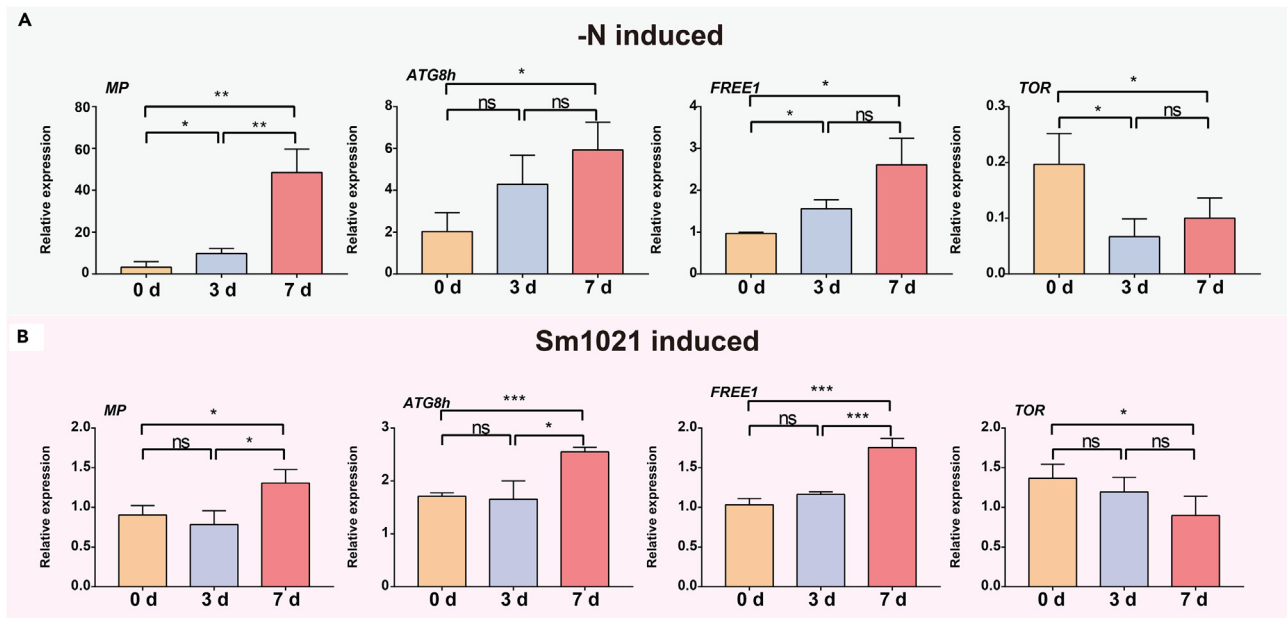


Figure 4. Expression pattern of autophagy related genes

(A and B) Transcript level of *MP*, *ATG8h*, *FREE1* and *TOR* in *Medicago* wild type roots with N starvation treated for 0 to 7 days (A) and induced by *Sm1021* treated for 0 to 7 days (B). Data are mean \pm SD (n = 3). *p < 0.05, **p < 0.01, ***p < 0.001 (Student's t test).

formation of nodules (Figure S6A). The number and density of infection threads and nodule primordia were significantly lower in the *mp* mutant than in the WT (Figures S6B–S6E). So MtMP affected the formation of infection threads and nodule primordia. Expression of nodulation marker genes, including Nodule inception (*NIN*), Interacting protein of DMI3 (*IPD3*), and nuclear factor Y, subunit A1 (*NF-YA1*) was reduced in *mp* mutant nodules at 7 days and 14 days after inoculation with *Sm1021* (Figures 5E–5G). Next, we examined the phenotype at 21 dpi, and the number of nodules in the *mp* mutants was also significantly lower than that in the WT at 21 dpi (Figure S6F). The most important is that the mature nodules of the *mp* mutant had significantly lower nitrogenase activity and significantly reduced nodule fresh weight and nodule size compared to WT plants (Figures 5A–5D). We also observed that WT nodules were pink in color (Figure 5A). Pink nodules have better nitrogen fixation capacity.^{24,25} In contrast, the nodules of the *mp* mutant were lighter in color, and these results imply that the nodules of the *mp* mutant were poorly developed and had a reduced nitrogen fixation capacity. In summary, MtMP mainly promotes the nitrogen fixation capacity of mature nodules.

MtMP affects mitophagy in the nodule infection zone

During nodule formation, the mitochondrial morphology is swollen and its functionality declines in infection zone.²⁶ Autophagy may be required to participate in the degradation of these mitochondria with reduced function during the transformation of infected cells into nitrogen-fixing cells. VDAC was used as a mitochondrial marker of immunostaining to clarify the mitochondrial number in root nodules. Compared with WT plants, *mp* mutants had stronger fluorescence intensity in the infection zone (Figures 6A and 6C). By counting the number of fluorescent spots (mitochondria) in the cells of the infection zone, we found that *mp* mutants had significantly more mitochondria than the WT (Figures 6B and 6D). The mitochondrial number of WT and *mp* mutant nodules was also detected with immunoblot. The degradation of mitochondrial markers (VDAC and COXII) is blocked in autophagy-defective mutants.²⁷ We found that VDAC and COXII accumulated in *mp* mutant nodules (Figure 6E), but the difference is not as pronounced as in the immunostaining counts. We speculate that the proteins used for immunoblotting were extracted from whole nodules, *MtMP* is expressed in cells in the infection zone of nodules (Figure 1M). The results show that MtMP is involved in the mitophagy of cells in the infection zone. The inhibition of mitophagy in the *mp* mutant may in turn inhibit the conversion of cells in the infection zone into cells in the nitrogen-fixing zone, thereby affecting nodule size, color, and nitrogen-fixing capacity.

We also examined autophagy under carbon starvation, the yellowing of WT and *mp* mutant leaves was consistent between 0 and 6 days of carbon starvation. The chloroplast marker TIC was quickly depleted under carbon starvation in both WT and *mp* mutant leaves. But there was no significant difference in chloroplast marker content between WT and *mp* mutant (Figure S7). The results indicated that MP was not involved in autophagy induced by carbon starvation.

DISCUSSION

Autophagy is crucial in the tissue and cell differentiation and development of both mammals and invertebrates. Autophagy has been found to be involved in directed differentiation in a variety of tissues and cells, including embryonic, stem and immune cells.^{28,29} During cellular differentiation,

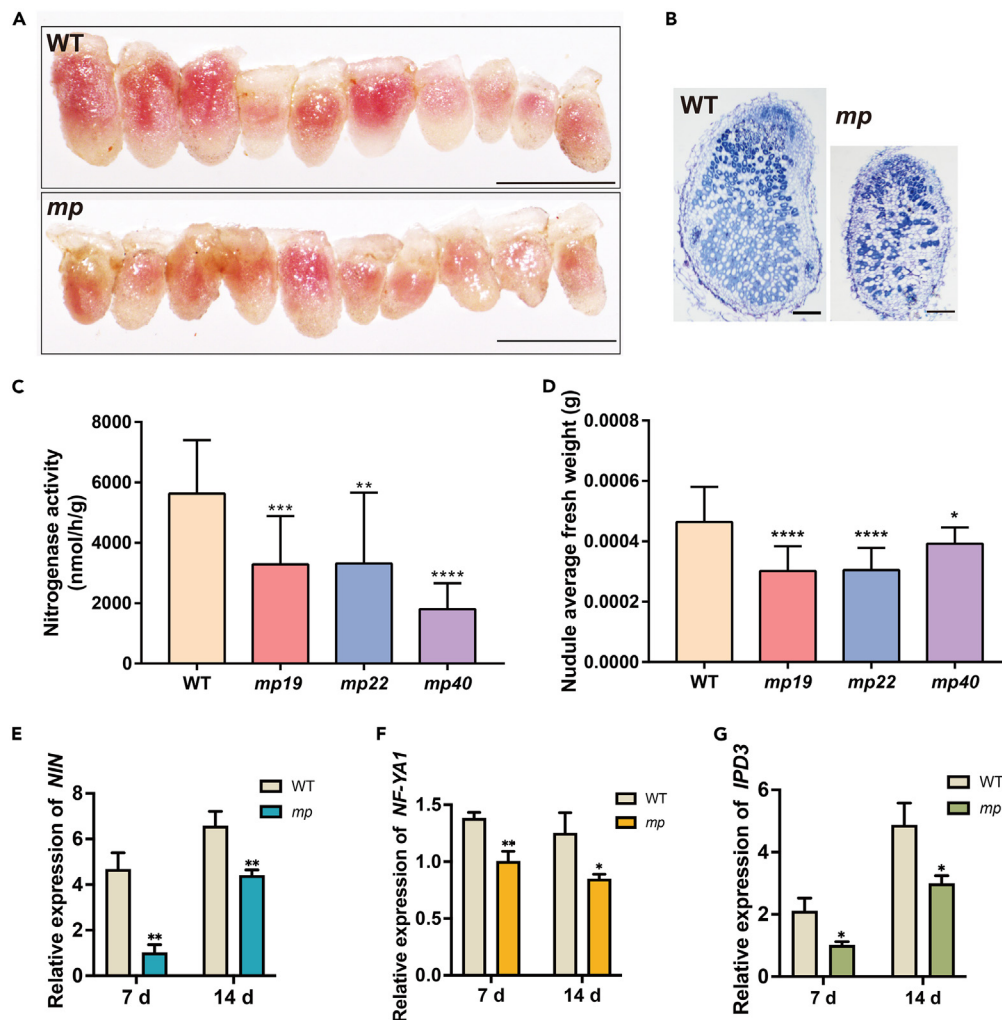


Figure 5. MP affects nitrogen fixing capacity of nodules

(A) Phenotype of nodule of 21dpi WT and *mp* mutant plants (Bar = 1 mm).

(B) Microscopic phenotype of nodule of 21dpi WT and *mp* mutant plants (Bar = 100 μ m).

(C) Nitrogenase activity of 21dpi WT, *mp19*, *mp22*, *mp40* plants. Data are presented as mean \pm SD for 15 individual plants. ** $p < 0.01$, *** $p < 0.001$, **** $p < 0.0001$, (Student's *t* test).

(D) Nodule average fresh weight of 21dpi WT, *mp19*, *mp22*, *mp40* plants. Data are presented as mean \pm SD for 15 individual plants. * $p < 0.05$, **** $p < 0.0001$, (Student's *t* test).

(E–G) Transcript levels of multiple nodulation marker genes (*NIN*, *NF-YA1* and *IPD3*) in WT and *mp* mutant plants at 7 dpi and 14 dpi induced by *Sm1021*. Data are mean \pm SD ($n = 3$). * $p < 0.05$, ** $p < 0.01$ (Student's *t* test).

cells transition from an undifferentiated state to a differentiated state in a complex regulatory manner. This process requires the degradation of obsolete proteins to allow the synthesis of new proteins required for cellular transition. Autophagy degrades these obsolete or redundant protein complexes to provide substrates for the synthesis of new proteins required for cellular activities associated with morphogenesis.³⁰

During cellular transformation involving autophagy, MtMP can dephosphorylate PtdIns3P on autophagosomes to promote autophagy, and studies in yeast have shown that the removal of PtdIns3P from autophagosomes is required for autophagosome fusion with vacuoles. It is unknown whether autophagy requires dephosphorylation of PtdIns3P in plants. In this study, we found that PtdIns3P on autophagosomes inhibits the fusion with vacuoles under certain conditions. We also examined autophagy under carbon starvation. There was no significant difference in chloroplast marker content between WT and *mp* mutant (Figure S7), which indicates that MtMP does not participate in all types of autophagy. This result may indicate that autophagy is very finely regulated. In future studies, resolving these finely regulated processes will be important for understanding organ, tissue and cellular remodeling and differentiation.

Mitochondria are dynamic organelles that constantly adapt to environmental changes. Severe energy stress can cause mitochondria dysfunction and pathological swelling.²⁶ When mitochondrial function is impaired, the production of more free radicals than energy

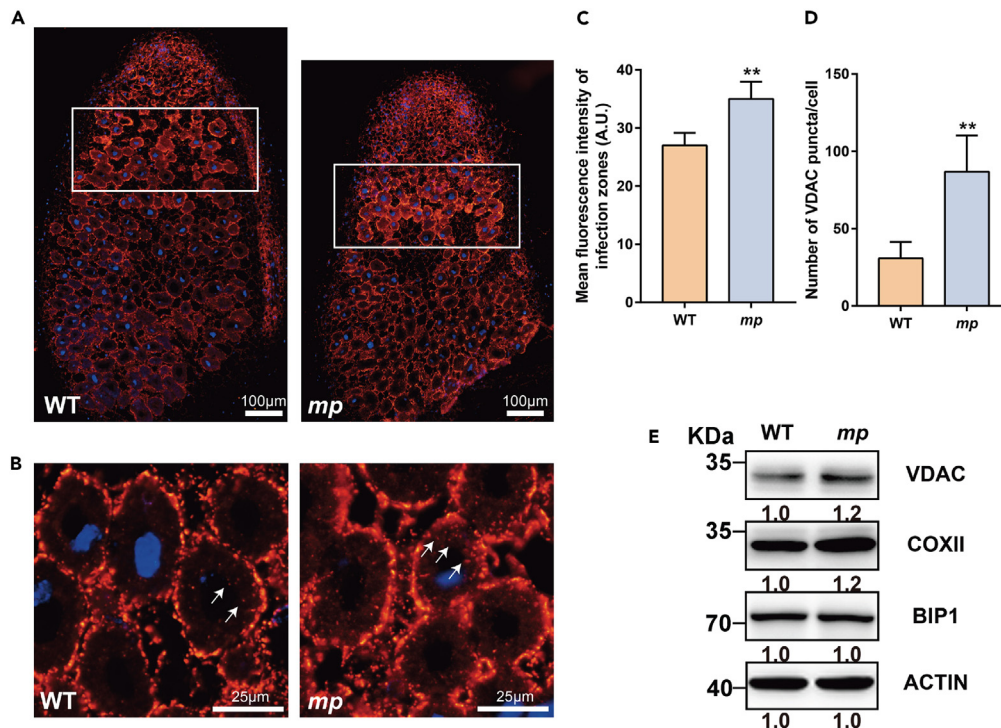


Figure 6. MP promotes mitochondrial degradation in nodules

(A) Immunostaining of mature nodules of WT and *mp* mutant plants. White boxes mean infection zone of WT and *mp* mutant nodules. Blue fluorescence (DAPI) is cell nucleus. Red fluorescence (anti-VDAC) is mitochondria (Bar = 100 μ m). (B) Enlarge view of infection zone of WT and *mp* mutant nodules. White arrows mitochondria of WT and *mp* mutant infection zones of nodules (Bar = 25 μ m). (C) Mean fluorescence intensity of infection zones. ** $p < 0.01$ (Student's *t* test). (D) The number of VDAC puncta per cell in WT and *mp* mutant plants. ** $p < 0.01$ (Student's *t* test). (E) Immunoblot of mature nodules of WT and *mp* mutant plants. ACTIN was used as internal reference gene.

leads to increasing oxidative pressure, and mitophagy begins in cells.³¹ Mitophagy provides carbon skeletons and nitrogen for cells.^{27,32} During uncoupler treatment, the damaged mitochondria are selectively engulfed by autophagosomes that are labeled by ATG8 proteins in an ATG5-dependent manner in *Arabidopsis*,³³ suggesting that ATG8 is involved in the mitophagy in plants. For cells in the nodule infection zone, it was observed that the mitochondria became larger and longer and presented more cristae,³⁴ indicating that the mitochondria in plant cells were stressed during the infection of rhizobia into plant cells. MtMP was expressed specifically in the nodule infection zone. When mitochondrial function was impaired, MtMP participate in mitophagy (Figure 6) and recover carbon skeletons and nitrogen from mitochondria, which may constitute a source of substances for the formation of bacteroids. In the MP deletion mutants, mitochondria accumulated in the infection region (Figure 6), the degradation and regeneration cycle of mitochondria in the cells were disrupted, and the intracellular material supply was not in balance, which affected nodule development and resulted in a decrease in nodule weight. This affected the nitrogen-fixation ability of the nodules, which was characterized by a decrease in nitrogenase activity (Figure 6). Under nitrogen starvation, legumes shift from normal growth to symbiotic nodulation, which is a complex biological change.¹⁶ During the development of mature nodules, most of the cells in the nitrogen-fixing zone are transformed from cells in the infection zone.¹⁶ Cells in the infection zone need to undergo rhizobial transformation into bacteroids.³⁵ MtMP is involved in mitophagy in the infection zone and may help transform the infected cells into nitrogen-fixing cells. In conclusion, mitophagy plays a crucial role in symbiotic nitrogen fixation.

Based on the previous research results on the mechanism of mitophagy in animals, yeast and plants,^{1,32,36,37} we proposed a putative model of mitophagy in the nodule infection zone (Figure 7). Under the induced conditions, TOR and ATG1, important regulators upstream of autophagy, initiate the assembly of the pre-autophagosomal structure (PAS). A variety of autophagy-related proteins are involved in this mid-autophagy process, including PI3K, which phosphorylates PtdIns on the PAS to generate PtdIns3P. Moreover, some ATG proteins help ATG8 attach to PE and anchor to the PAS.³⁸ Eventually, the PAS bends and wraps into an autophagy vesicle with the help of proteins such as SH3P2 for transport toward the vacuole. downstream of autophagy, PtdIns3P on the autophagosome needs to be dephosphorylated by MP and fused with vacuoles with the help of the ESCRT complex. Hydrolases in the vacuoles hydrolyze the cargo into amino acids, sugars, lipids and other basic substances.¹ Cells can recycle these basic C and N sources as well as energetic materials to synthesize new functional proteins and organelles.

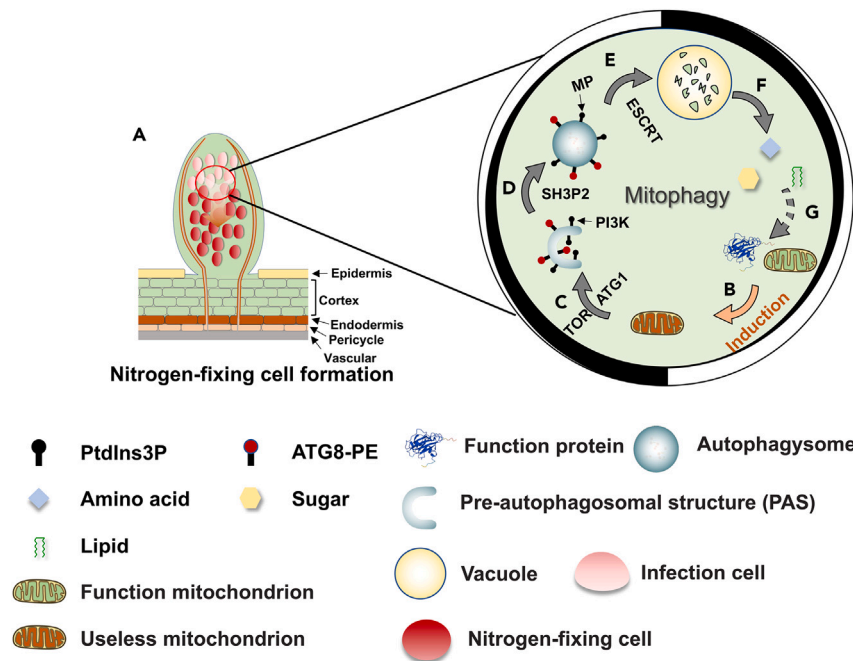


Figure 7. The model of mitophagy in the nodule infection zone

(A) The infection cells transfer to nitrogen-fixing cells in mature nodules.

(B) Induction of autophagy.

(C) TOR and ATG1 participate the upstream of autophagy.

(D) Formation of pre-autophagosomal structure (PAS). PI3K phosphorylates PtdIns to produce PtdIns3P. SH3P2 assists in the transformation of PAS into autophagosomes.

(E) MP dephosphorylate PtdIns3P for maturation of autophagosome for fusing with vacuoles assisted by ESCRT.

(F) Autophagosomes fuse with vacuoles where its cargo is degraded by resident hydrolases. These digestion products can be transported back to the cytosol for re-use.

(G) The digestion products can resynthesis function proteins and organelles. The middle circle is a simplified diagram of ouroboros that represents the inner impetus and self-perpetuating.

Limitations of the study

Under low nitrogen conditions, legumes transition from normal growth to symbiotic nodulation, which is a complex biological change.¹⁶ There are four main processes of symbiotic nodulation between legume and rhizobia, each of which involves cell differentiation or morphological transformation. Our research found that MtMP promotes the nitrogen fixation capacity of mature nodules. MtMP participate in mitophagy and recover carbon skeletons and nitrogen from mitochondria, which may constitute a source of substances for the formation of bacteroid and may help infected cells transform into nitrogen-fixing cells. At the same time, we also found that MtMP affects the early events of nodule formation, such as the number of infection threads and nodule primordia, but it is still unclear how MtMP affects the formation of infection threads and nodule primordia. In future research, further investigation of these regulatory processes will be critical to understanding the organogenesis of nodules.

STAR★METHODS

Detailed methods are provided in the online version of this paper and include the following:

- [KEY RESOURCES TABLE](#)
- [RESOURCE AVAILABILITY](#)
 - Lead contact
 - Material availability
 - Data and code availability
- [EXPERIMENTAL MODEL AND STUDY PARTICIPANT DETAILS](#)
- [METHOD DETAILS](#)
 - RT-qPCR
 - *Agrobacterium rhizogenes* transformation in hairy roots
 - Generation of constructs and transgenic lines

- ITs, primordia, and nodulation phenotype assays
- Subcellular localization of MP
- GUS staining analysis
- GFP cleavage assays
- Phosphatase activity assays
- Protein lipid overlay assay
- Nodule immunofluorescence assays
- Shoot carbon hungry assays
- **QUANTIFICATION AND STATISTICAL ANALYSIS**
- Accession numbers

SUPPLEMENTAL INFORMATION

Supplemental information can be found online at <https://doi.org/10.1016/j.isci.2023.107752>.

ACKNOWLEDGMENTS

We thank Prof. Fulvio Reggiori (University of Groningen) for his generous gift of yeast strains in this work. This work was supported by grants from National Natural Science Foundation of China (32070272) and National Key Research and Development Program of China (2022YFA0912100).

AUTHOR CONTRIBUTIONS

J.D. conceived the study and designed the experiments. Q.X., C.S., J.L., C.L., and Q.Y. performed the experiments. C.S., Q.L., P.L., D.G., and L.Z. analyzed the data. C.S., Q.X., J.D., and T.W. wrote the manuscript.

DECLARATION OF INTERESTS

The authors declare no competing interests.

Received: May 18, 2022

Revised: June 7, 2023

Accepted: August 24, 2023

Published: September 15, 2023

REFERENCES

1. Marshall, R.S., and Vierstra, R.D. (2018). Autophagy: The Master of Bulk and Selective Recycling. *Annu. Rev. Plant Biol.* 69, 173–208.
2. Wang, P., Mugume, Y., and Bassham, D.C. (2018). New advances in autophagy in plants: Regulation, selectivity and function. *Semin. Cell Dev. Biol.* 80, 113–122.
3. Yang, M., Ismayil, A., and Liu, Y. (2020). Autophagy in Plant-Virus Interactions. *Annu. Rev. Virol.* 7, 403–419.
4. Suttangkakul, A., Li, F., Chung, T., and Vierstra, R.D. (2011). The ATG1/ATG13 protein kinase complex is both a regulator and a target of autophagic recycling in *Arabidopsis*. *Plant Cell* 23, 3761–3779.
5. Zhuang, X., Chung, K.P., Cui, Y., Lin, W., Gao, C., Kang, B.H., and Jiang, L. (2017). ATG9 regulates autophagosome progression from the endoplasmic reticulum in *Arabidopsis*. *Proc. Natl. Acad. Sci. USA* 114, E426–E435.
6. Qi, H., Xia, F.N., Xie, L.J., Yu, L.J., Chen, Q.F., Zhuang, X.H., Wang, Q., Li, F., Jiang, L., Xie, Q., and Xiao, S. (2017). TRAF Family Proteins Regulate Autophagy Dynamics by Modulating AUTOPHAGY PROTEIN6 Stability in *Arabidopsis*. *Plant Cell* 29, 890–911.
7. Zhuang, X., Wang, H., Lam, S.K., Gao, C., Wang, X., Cai, Y., and Jiang, L. (2013). A BAR-domain protein SH3P2, which binds to phosphatidylinositol 3-phosphate and ATG8, regulates autophagosome formation in *Arabidopsis*. *Plant Cell* 25, 4596–4615.
8. Gao, C., Zhuang, X., Cui, Y., Fu, X., He, Y., Zhao, Q., Zeng, Y., Shen, J., Luo, M., and Jiang, L. (2015). Dual roles of an *Arabidopsis* ESCRT component FREE1 in regulating vacuolar protein transport and autophagic degradation. *Proc. Natl. Acad. Sci. USA* 112, 1886–1891.
9. Tsujita, K., Itoh, T., Ijuin, T., Yamamoto, A., Shisheva, A., Laporte, J., and Takenawa, T. (2004). Myotubularin regulates the function of the late endosome through the gram domain-phosphatidylinositol 3,5-bisphosphate interaction. *J. Biol. Chem.* 279, 13817–13824.
10. Mruk, D.D., and Cheng, C.Y. (2011). The myotubularin family of lipid phosphatases in disease and in spermatogenesis. *Biochem. J.* 433, 253–262.
11. Cebollero, E., van der Vaart, A., and Reggiori, F. (2012). Understanding phosphatidylinositol-3-phosphate dynamics during autophagosome biogenesis. *Autophagy* 8, 1868–1870.
12. Cebollero, E., van der Vaart, A., Zhao, M., Rieter, E., Klionsky, D.J., Helms, J.B., and Reggiori, F. (2012). Phosphatidylinositol-3-phosphate clearance plays a key role in autophagosome completion. *Curr. Biol.* 22, 1545–1553.
13. Parrish, W.R., Stefan, C.J., and Emr, S.D. (2004). Essential role for the myotubularin-related phosphatase Ymr1p and the synaptojanin-like phosphatases Sjl2p and Sjl3p in regulation of phosphatidylinositol 3-phosphate in yeast. *Mol. Biol. Cell* 15, 3567–3579.
14. Ding, Y., Ndamukong, I., Zhao, Y., Xia, Y., Riethoven, J.J., Jones, D.R., Divecha, N., and Avramova, Z. (2012). Divergent functions of the myotubularin (MTM) homologs AtMTM1 and AtMTM2 in *Arabidopsis thaliana*: evolution of the plant MTM family. *Plant J.* 70, 866–878.
15. Nagpal, A., Hassan, A., Ndamukong, I., Avramova, Z., and Baluška, F. (2018). Myotubularins, PtdIns5P, and ROS in ABA-mediated stomatal movements in dehydrated *Arabidopsis* seedlings. *Funct. Plant Biol.* 45, 259–266.
16. Roy, S., Liu, W., Nandety, R.S., Crook, A., Mysore, K.S., Pislariu, C.I., Frugoli, J., Dickstein, R., and Udvardi, M.K. (2020). Celebrating 20 Years of Genetic Discoveries in Legume Nodulation and Symbiotic Nitrogen Fixation. *Plant Cell* 32, 15–41.
17. Estrada-Navarrete, G., Cruz-Mireles, N., Lascano, R., Alvarado-Affantranger, X., Hernández-Barrera, A., Barraza, A., Olivares, J.E., Arthikala, M.K., Cárdenas, L., Quinto, C., and Sanchez, F. (2016). An

- Autophagy-Related Kinase Is Essential for the Symbiotic Relationship between *Phaseolus vulgaris* and Both Rhizobia and Arbuscular Mycorrhizal Fungi. *Plant Cell* 28, 2326–2341.
18. Nanjareddy, K., Blanco, L., Arthikala, M.K., Alvarado-Affantranger, X., Quinto, C., Sánchez, F., and Lara, M. (2016). A Legume TOR Protein Kinase Regulates Rhizobium Symbiosis and Is Essential for Infection and Nodule Development. *Plant Physiol.* 172, 2002–2020.
 19. Doerks, T., Strauss, M., Brendel, M., and Bork, P. (2000). GRAM, a novel domain in glucosyltransferases, myotubularins and other putative membrane-associated proteins. *Trends Biochem. Sci.* 25, 483–485.
 20. Zhu, F., Ye, Q., Chen, H., Dong, J., and Wang, T. (2021). Multigene editing reveals that MtCEP1/2/12 redundantly control lateral root and nodule number in *Medicago truncatula*. *J. Exp. Bot.* 72, 3661–3676.
 21. Chung, T. (2019). How phosphoinositides shape autophagy in plant cells. *Plant Sci.* 281, 146–158.
 22. Simon, M.L.A., Platre, M.P., Assil, S., van Wijk, R., Chen, W.Y., Chory, J., Dreux, M., Munnik, T., and Jaillais, Y. (2014). A multi-colour/multi-affinity marker set to visualize phosphoinositide dynamics in *Arabidopsis*. *Plant J.* 77, 322–337.
 23. Chiarugi, P., Marzocchini, R., Raugei, G., Pazzagli, C., Berti, A., Camici, G., Manao, G., Cappugi, G., and Ramponi, G. (1992). Differential role of four cysteines on the activity of a low Mr phosphotyrosine protein phosphatase. *FEBS Lett.* 310, 9–12.
 24. Gauthier-Coles, C., White, R.G., and Mathesius, U. (2018). Nodulating Legumes Are Distinguished by a Sensitivity to Cytokinin in the Root Cortex Leading to Pseudonodule Development. *Front. Plant Sci.* 9, 1901.
 25. Kim, M., Chen, Y., Xi, J., Waters, C., Chen, R., and Wang, D. (2015). An antimicrobial peptide essential for bacterial survival in the nitrogen-fixing symbiosis. *Proc. Natl. Acad. Sci. USA* 112, 15238–15243.
 26. Javadov, S., Chapa-Dubocq, X., and Makarov, V. (2018). Different approaches to modeling analysis of mitochondrial swelling. *Mitochondrion* 38, 58–70.
 27. Li, F., Chung, T., and Vierstra, R.D. (2014). AUTOPHAGY-RELATED11 plays a critical role in general autophagy- and senescence-induced mitophagy in *Arabidopsis*. *Plant Cell* 26, 788–807.
 28. Hu, Y.X., Han, X.S., and Jing, Q. (2019). Autophagy in Development and Differentiation. *Adv. Exp. Med. Biol.* 1206, 469–487.
 29. Wang, L., Das, J.K., Kumar, A., Peng, H.Y., Ren, Y., Xiong, X., Yang, J.M., and Song, J. (2021). Autophagy in T-cell differentiation, survival and memory. *Immunol. Cell Biol.* 99, 351–360.
 30. Offei, E.B., Yang, X., and Brand-Saberi, B. (2018). The role of autophagy in morphogenesis and stem cell maintenance. *Histochem. Cell Biol.* 150, 721–732.
 31. Szczepanowska, K., and Trifunovic, A. (2022). Mitochondrial matrix proteases - quality control and beyond. *FEBS J.* 289, 7128–7146.
 32. Nakamura, S., Hagihara, S., and Izumi, M. (2021). Mitophagy in plants. *Biochim. Biophys. Acta. Gen. Subj.* 1865, 129916.
 33. Ma, J., Liang, Z., Zhao, J., Wang, P., Ma, W., Mai, K.K., Fernandez Andrade, J.A., Zeng, Y., Grujic, N., Jiang, L., et al. (2021). Friendly mediates membrane depolarization-induced mitophagy in *Arabidopsis*. *Curr. Biol.* 31, 1931–1944.e4.
 34. Werner, D., and Mörschel, E. (1978). Differentiation of nodules of *Glycine max*: Ultrastructural studies of plant cells and bacteroids. *Planta* 141, 169–177.
 35. Ogden, A.J., Gargouri, M., Park, J., Gang, D.R., and Kahn, M.L. (2017). Integrated analysis of zone-specific protein and metabolite profiles within nitrogen-fixing *Medicago truncatula*-*Sinorhizobium medicae* nodules. *PLoS One* 12, e0180894.
 36. Li, W., He, P., Huang, Y., Li, Y.F., Lu, J., Li, M., Kurihara, H., Luo, Z., Meng, T., Onishi, M., et al. (2021). Selective autophagy of intracellular organelles: recent research advances. *Theranostics* 11, 222–256.
 37. Tang, J., and Bassham, D.C. (2018). Autophagy in crop plants: what's new beyond *Arabidopsis*? *Open Biol.* 8, 180162.
 38. Nair, U., Yen, W.L., Mari, M., Cao, Y., Xie, Z., Baba, M., Reggiori, F., and Klionsky, D.J. (2012). A role for Atg8-PE deconjugation in autophagosome biogenesis. *Autophagy* 8, 780–793.
 39. Zhou, H., Lin, H., Chen, S., Becker, K., Yang, Y., Zhao, J., Kudla, J., Schumaker, K.S., and Guo, Y. (2014). Inhibition of the *Arabidopsis* salt overly sensitive pathway by 14-3-3 proteins. *Plant Cell* 26, 1166–1182.
 40. Gonzalez-Rizzo, S., Crespi, M., and Frugier, F. (2006). The *Medicago truncatula* CRE1 cytokinin receptor regulates lateral root development and early symbiotic interaction with *Sinorhizobium meliloti*. *Plant Cell* 18, 2680–2693.
 41. Qin, L., Zhou, Z., Li, Q., Zhai, C., Liu, L., Quilichini, T.D., Gao, P., Kessler, S.A., Jaillais, Y., Datla, R., et al. (2020). Specific Recruitment of Phosphoinositide Species to the Plant-Pathogen Interfacial Membrane Underlies *Arabidopsis* Susceptibility to Fungal Infection. *Plant Cell* 32, 1665–1688.
 42. Martin, B., Pallen, C.J., Wang, J.H., and Graves, D.J. (1985). Use of fluorinated tyrosine phosphates to probe the substrate specificity of the low molecular weight phosphatase activity of calcineurin. *J. Biol. Chem.* 260, 14932–14937.
 43. Schaletzky, J., Dove, S.K., Short, B., Lorenzo, O., Clague, M.J., and Barr, F.A. (2003). Phosphatidylinositol-5-phosphate activation and conserved substrate specificity of the myotubularin phosphatidylinositol 3-phosphatases. *Curr. Biol.* 13, 504–509.
 44. Han, X., Yang, Y., Zhao, F., Zhang, T., and Yu, X. (2020). An improved protein lipid overlay assay for studying lipid-protein interactions. *Plant Methods* 16, 33.
 45. Weaver, L.M., and Amasino, R.M. (2001). Senescence is induced in individually darkened *Arabidopsis* leaves, but inhibited in whole darkened plants. *Plant Physiol.* 127, 876–886.

STAR★METHODS

KEY RESOURCES TABLE

REAGENT or RESOURCE	SOURCE	IDENTIFIER
Antibodies		
anti-GFP	Proteintech	Cat#66002-1-Ig; RRID:AB_11182611
anti-NPTII	Abcam	Cat#ab60018; RRID:AB_944399
anti-VDAC	Agrisera	Cat#AS07212; RRID:AB_1031829
anti-COXII	Agrisera	Cat#AS04053; RRID:AB_347493
anti-BIP1	Agrisera	Cat#AS09481; RRID:AB_1832007
anti-His	Proteintech	Cat#66005-1-Ig; RRID:AB_11232599
anti-ACTIN	CWBIO	Cat#CW0096; RRID:AB_2665433
goat anti-rabbit IgG-AF594 secondary antibodies	QualiYard	Cat#QYB082
goat anti-mouse IgG secondary antibodies	seracare KPL	Cat#5220-0341; RRID:AB_2891080
Bacterial and virus strains		
<i>Sinorhizobium meliloti</i> 1021	N/A	N/A
<i>Agrobacterium rhizogenes</i> ARqua1	N/A	N/A
<i>Agrobacterium tumefaciens</i> EHA105	N/A	N/A
<i>Escherichia coli</i> TOP10	N/A	N/A
<i>Escherichia coli</i> Rosetta (DE3)	TIANGEN	Cat#CB108
Chemicals, peptides, and recombinant proteins		
4',6-diamidino-2-phenylindole (DAPI)	Sigma	Cat#28718-90-3
X-gluc	Sigma	Cat#B5285
agarose	Sigma	Cat#A9414
Trizol	Invitrogen	Cat#16695-018
PtdIns3P	Avanti Polar Lipids	Cat#850150
HiScript II 1st strand cDNA synthesis kit	Vazyme	Cat#R211
SYBR qPCR mix	Vazyme	Cat#Q712
His-MBP-MP (myotube-related enzyme active domain)	This paper	N/A
His-MBP-AtMTM1	This paper	N/A
His-MBP-MPN (PH-like domain)	This paper	N/A
Critical commercial assays		
Phosphatase kit	Echelon Biosciences	Cat#JJ-052208 http://www.echelon-inc.com/
Experimental models: Organisms/strains		
R108	N/A	N/A
<i>mp22/mp19/mp40</i> (CRISPR/Cas9)	This paper	N/A
GFP-MtATG8	This paper	N/A
<i>ProMP::GUS</i>	This paper	N/A
yeast <i>ymr1Δ</i> mutant strain	Cebollero et al., 2012 ¹²	N/A
yeast <i>ymr1Δ+ProScYmr1::Ymr1</i>	This paper	N/A
yeast <i>ymr1Δ+ProScYmr1::MtMP</i>	This paper	N/A

(Continued on next page)

Continued

REAGENT or RESOURCE	SOURCE	IDENTIFIER
Oligonucleotides		
See Table S1	N/A	N/A
Recombinant DNA		
Pro35S::GFP-MtMP	This paper	N/A
Pro35S::mCherry-MtATG8	This paper	N/A
Pro35S::mCherry-2xFYVE	This paper	N/A
GFP-ScATG8	This paper	N/A
Software and algorithms		
GraphPad Prism9	Open source	https://www.graphpad.com
ImageJ	Open source	https://ImageJ.nih.gov/ij/

RESOURCE AVAILABILITY**Lead contact**

Further information and requests for resources and reagents should be directed to and will be fulfilled by the lead contact, Jiangli Dong (dongjl@cau.edu.cn).

Material availability

Materials generated in this study are available upon request. For further details contact the [lead contact](#).

Data and code availability

- All data reported in this paper will be shared by the [lead contact](#) upon request.
- This paper does not report original code.
- Any additional information required to reanalyze the data reported in this paper is available from the [lead contact](#) upon request.

EXPERIMENTAL MODEL AND STUDY PARTICIPANT DETAILS

R108 *M. truncatula* plants were used in this study. Seeds were treated with 98% (v/v) H₂SO₄ for 8 min, washed three times with water, sterilized with 5% (v/v) sodium hypochlorite for 12 min, and then washed six times with sterile water. The seeds were then placed on the surface of 0.8% (w/v) agarose media and stratified at 4°C for 3 days, after which they were germinated at 24°C in the dark. All the plants were subsequently grown in a greenhouse (22°C temperature, 16/8 h light/dark photoperiod, 100 to 150 μmol m²/s light intensity provided by a white fluorescent lamp, and 60 to 70% humidity). For seed production, plants were grown in a soil:vermiculite (1:3, v/v) mixture. For nodulation, plants were grown in a perlite:vermiculite (2:5, v/v) mixture soaked in N-deprived Fåhræus media for 1 week and then inoculated with *Sm1021* rhizobia resuspended in liquid Fåhræus media (OD₆₀₀ nm = 0.05). For N-starvation experiments, plants were grown on plates of Fåhræus media supplemented with 1.5% (w/v) agarose covered with seed germination paper (Anchor Paper) or in liquid Fåhræus media with or without N.

METHOD DETAILS**RT-qPCR**

RT-qPCR was used to confirm RNA-seq expression data for selected genes related to autophagy and nodulation. To detect the expression of autophagy related genes, RNA was extracted with Trizol reagent from roots of R108 treated with nitrogen hungry or inoculated with *Sm1021* for 0, 3, and 7 days. To detect the expression of nodulation related marker genes, RNA was extracted with Trizol reagent from nodules of R108 and *mp* mutants which were grown in Fåhræus medium for 7 days and then inoculated with *Sm1021* for 7 days and 14 days.

First-strand cDNA was synthesized with 1 μg of total RNA using HiScript II 1st strand cDNA synthesis kit. SYBR qPCR mix was used as well as the CFX-96 real-time system (Bio-Rad). Gene expression was calculated using the 2^{-ΔΔCT} method. *MtACTIN4A* and *MtRBP1* was used as a reference gene. The primers used in this experiment are listed in Table S1.

***Agrobacterium rhizogenes* transformation in hairy roots**

The full-length ATG8 and 2xFYVE coding sequences (CDS) overlapping with GFP or mCherry sequences were cloned into a pCambia-1307-FLAG-HA vector,³⁹ an FLAG-HA tag was fused to the C-terminal end of the genes, and *Agrobacterium rhizogenes* ARqua1 strains⁴⁰ expressing either a Pro35S::GFP-ATG8-FLAG-HA construct or a Pro35S::mCherry-2xFYVE-FLAG-HA construct was used to transform R108 and *mp* mutants. In brief, seedlings were incubated together with ARqua1 for 1 week in half-strength Murashige and Skoog media (without sucrose (Suc))

at 20°C, transferred to new media (with 20 g/L Suc and 3 mM MES, pH 5.8) for 1 week at 24°C, and then transferred to a plate with freshly solidified Fåhræus media (without Suc) covered with seed germination paper. Three weeks later, the roots of the transgenic plants were subjected to fluorescence observations.

Generation of constructs and transgenic lines

A stable *mp* mutant was generated based on the CRISPR/Cas9 system, as reported by Zhu et al.²⁰ Briefly, a site (CCCTGTCA AATGACTTGTTGG) was selected from the 7th MtMP exon as well as the *MtU6-1* promoter in the pCBC-1 vector. Mutations in MPs were detected in individual transgenic plants by sequencing. The MP promoter (the 2.5 kb region upstream of ATG) was cloned into a pCAMBIA-1381 vector, after which the resulting *ProMP::GUS* vector was stably transformed into R108 cells.

The transformation protocol is briefly described here. Constructs were transferred into the EHA105 strain, which were subsequently cultured in yeast extract beef (YEB) liquid media until the OD₆₀₀ reached 0.6. The culture was then centrifuged and gently resuspended in SH3 α liquid media (OD₆₀₀ = 0.6). Leaves of 3- to 4-week-old *in vitro* plants were chosen, cut into pieces and put into an *Agrobacterium* mixture, after which a vacuum was applied to the leaf explants for 30 min. The leaf explants were transferred to sterile paper to remove the bacterial solution and then placed on solid SH3 α media without antibiotics; the explants were subsequently allowed to grow for 3 days in the dark (at 24°C). The leaf explants were then transferred onto SH3 α media (supplemented with 50 mg/L hygromycin and 200 mg/L timentin) and cultured for 6 weeks in the dark at 24°C (during which time they were transferred to new SH3 α media every 2 weeks). The leaf explants were then transferred to solid SH9 media for further cultivation (4–6 weeks). Finally, the plantlets were transferred to 1/2-strength MS media (1.5% Suc, 0.8% agar) to induce rooting.

ITs, primordia, and nodulation phenotype assays

Plants were grown in a perlite:vermiculite (2:5, v/v) mixture soaked in N-deprived Fåhræus media for 1 week and then inoculated with *Sm1021* rhizobia for 3 weeks before the nodulation phenotype assays were performed. To determine the IT and primordium phenotypes, the plants were inoculated with *Sm1021* rhizobia carrying a *ProHemA::LACZ* fusion construct for 5 days before X-Gal staining, which was performed as previously described by Gonzalez-Rizzo et al.⁴⁰

Subcellular localization of MP

For the subcellular localization of MP, the full-length MP protein was cloned into a pCAMBIA-1307-*Pro35S::GFP* vector, and then *Pro35S::MP-GFP* was transiently coexpressed with a *Pro35S::mCherry-ATG8* autophagy marker or a *Pro35S::mCherry-2xFYVE*⁴¹ PtdIns3P marker in *Arabidopsis* protoplasts. Fluorescence was detected using an SP8 confocal microscope (Leica) at excitation and emission wavelengths of 488 and 495 to 545 nm, respectively, for GFP and 552 and 590 to 670 nm, respectively, for mCherry.

GUS staining analysis

For GUS staining analysis, the roots of transgenic plants were stained in a solution (pH 7.0) consisting of 10 mM EDTA disodium salt, 100 mM NaH₂PO₄, 0.5 mM K₄Fe (CN)₆, 0.5 mM K₃Fe (CN)₆, 0.1% Triton X-100, and 0.5 mg/mL X-gluc at 37°C for 12 h. The GUS staining patterns were then observed and photographed with an Olympus BX51 microscope. The GUS-stained roots were embedded in 3% (m/v) low-gelling-temperature agarose and sectioned at a thickness of 50 μ m using a Leica VT1000S instrument.

GFP cleavage assays

To evaluate autophagic flux, GFP-MtATG8 was expressed in WT plants and *mp* mutants via hairy root transformation. The total protein of the roots was extracted under N-starvation conditions. The protein extract was analyzed with anti-GFP, and free GFP was detected. To evaluate GFP cleavage when plants inoculated with rhizobia, GFP-MtATG8 stable plants inoculated with *Sm1021* after 7 days of N-starvation, and sampled from 0 days to 7 days of *Sm1021* inoculation to detect GFP cleavage. Like in plants, GFP-ScATG8 was expressed in the *ymr1 Δ* mutant strain, *ymr1 Δ +ProScYmr1::Ymr1* supplementation strain and *ymr1 Δ +ProScYmr1::MtMP* supplementation strain; the *ymr1 Δ* strain was a gift from Fulvio Reggiori.¹² Total protein was extracted under N-starvation conditions for 0 h, 2 h, 4 h and 6 h. ImageJ was used to perform gray value statistics.

Phosphatase activity assays

Phosphoinositide 3-phosphatase assays were performed using a malachite green assay^{42,43} with a standardized phosphatase kit according to the manufacturer's protocol. Recombinantly expressed and affinity column-purified His-MBP-tagged proteins were reacted with phosphoinositides (Echelon) as substrates. AtMTM1 phosphatase was used as a positive control. The truncated myotube-related enzyme active domain was used to purify the truncated MtMP recombinant protein. An AtMTM1 truncation vector and a His-MBP empty vector were used as controls.

Protein lipid overlay assay

Protein lipid overlay assay were performed as described previously.⁴⁴ Each PtdIns3P was spotted onto PVDF membrane and incubated at 23°C for 1 h to allow the chloroform to evaporate. The membrane was blocked at room temperature for 1 h in Tris-buffered saline (TBS)

containing 5% (w/v) skimmed milk powder, with shaking at 60 rpm. The membrane was incubated with 50 µg of recombinant His-MBP-MPN or His-MBP protein at 4°C for 16 h. The membrane was washed three times for 10 min each with TBST (containing 5% Tween 20), then incubated with anti-His monoclonal antibody at 23°C for 1 h. Goat anti-mouse IgG was used as a secondary antibody.

Nodule immunofluorescence assays

The nodules were placed in 4% paraformaldehyde in phosphate-buffered saline (PBS) (0.1 M; pH 7.4; Gibco) at 4°C for fixation. Paraffin embedding and paraffin sectioning were then performed. For VDAC immunofluorescence staining, sections were incubated together with rabbit anti-VDAC overnight at 4°C. After the unbound primary antibodies were removed, the sections were incubated with the corresponding goat anti-rabbit IgG-AF594 secondary antibodies for 1 h at 23°C, followed by nuclear staining with 4',6-diamidino-2-phenylindole (DAPI) for 5 min. The stained sections were then observed and imaged with an Olympus BX51 microscope. ImageJ was used to perform intensity statistics on the red fluorescence.

Shoot carbon hungry assays

Carbon hungry assays were performed as described previously⁴⁵ using seedlings grown for 4 weeks on soil at 21°C under LD conditions. The expanding third and fourth leaves were individually covered with aluminum foil, whereas the rest of the plant remained exposed to LD light conditions.

QUANTIFICATION AND STATISTICAL ANALYSIS

Statistical significance of the biological parameters was assessed using Student's t test. Statistical analyses were performed with the software GraphPad Prism9. The statistical parameters are reported in the figure legends.

Accession numbers

Sequence data from this article can be found in the *M. truncatula* genome database and the GenBank data library under accession numbers Medtr1g092570 (MtMP), Medtr7g096540 (MtATG8h), Medtr5g005380 (MtTOR), Medtr3g114080 (MtFREE1), Medtr5g099060 (MtNIN), Medtr1g056530 (MtNF-YA1), Medtr5g026850 (MtIPD3).